Tunable band-pass plasmonic waveguide filters with nanodisk resonators

Hua Lu, Xueming Liu,* Dong Mao, Leiran Wang, and Yongkang Gong

State Key Laboratory of Transient Optics and Photonics, Xi'an Institute of Optics and Precision Mechanics, Chinese Academy of Sciences, Xi'an 710119, China

**liuxm@opt.ac.cn*

Abstract: A novel and simple plasmonic filter based on metal-insulator-metal plasmonic waveguides with a nanodisk resonator is proposed and investigated numerically. By the resonant theory of disk-shaped nanocavity, we find that the resonance wavelengths can be easily manipulated by adjusting the radius and refractive index of the nanocavity, which is in good agreement with the results obtained by finite-difference time-domain (FDTD) simulations. In addition, the bandwidths of resonance spectra are tunable by changing the coupling distance between the nanocavity and waveguides. This result achieved by FDTD simulations can be accurately analyzed by temporal coupled mode theory. Our filters have important potential applications in high-density plasmonic integration circuits.

©2010 Optical Society of America

OCIS codes: (240.6680) Surface plasmons; (140.4780) Optical resonators; (130.7408) Wavelength filter; (130.3120) Integrated optics devices.

References and links

1. W. L. Barnes, A. Dereux, and T. W. Ebbesen, "Surface plasmon subwavelength optics," Nature **424**(6950), 824–830 (2003).
2. Q. Zhang, X. G. Huang, X. S. Lin, J. Tao, and X. P. Jin, "A subwavelength coupler-type MIM optical filter," Opt. Express **17**(9), 7549–7554 (2009).
3. C. Genet, and T. W. Ebbesen, "Light in tiny holes," Nature **445**(7123), 39–46 (2007).
4. C. Janke, J. G. Rivas, P. H. Bolivar, and H. Kurz, "All-optical switching of the transmission of electromagnetic radiation through subwavelength apertures," Opt. Lett. **30**(18), 2357–2359 (2005).
5. C. J. Min, P. Wang, C. C. Chen, Y. Deng, Y. H. Lu, H. Ming, T. Y. Ning, Y. L. Zhou, and G. Z. Yang, "All-optical switching in subwavelength metallic grating structure containing nonlinear optical materials," Opt. Lett. **33**(8), 869–871 (2008).
6. G. A. Wurtz, R. Pollard, and A. V. Zayats, "Optical bistability in nonlinear surface-plasmon polaritonic crystals," Phys. Rev. Lett. **97**(5), 057402 (2006).
7. B. Wang, and G. P. Wang, "Surface plasmon polariton propagation in nanoscale metal gap waveguides," Opt. Lett. **29**(17), 1992–1994 (2004).
8. G. Veronis, and S. Fan, "Bends and splitters in metal-dielectric-metal subwavelength plasmonic waveguides," Appl. Phys. Lett. **87**(13), 131102 (2005).
9. T. Nikolajsen, K. Leosson, and S. I. Bozhevolnyi, "Surface Plasmon polariton based modulators and switches operating at telecom wavelengths," Appl. Phys. Lett. **85**(24), 5833 (2004).
10. S. Randhawa, M. U. González, J. Renger, S. Enoch, and R. Quidant, "Design and properties of dielectric surface plasmon Bragg mirrors," Opt. Express **18**(14), 14496–14510 (2010).
11. S. Enoch, R. Quidant, and G. Badenes, "Optical sensing based on plasmon coupling in nanoparticle arrays," Opt. Express **12**(15), 3422–3427 (2004).
12. J. Park, H. Kim, and B. Lee, "High order plasmonic Bragg reflection in the metal-insulator-metal waveguide Bragg grating," Opt. Express **16**(1), 413–425 (2008).
13. Y. Gong, L. Wang, X. Hu, X. Li, and X. Liu, "Broad-bandgap and low-sidelobe surface plasmon polariton reflector with Bragg-grating-based MIM waveguide," Opt. Express **17**(16), 13727–13736 (2009).
14. J. W. Mu, and W. P. Huang, "A Low-Loss Surface Plasmonic Bragg Grating," J. Lightwave Technol. **27**(4), 436–439 (2009).
15. X. S. Lin, and X. G. Huang, "Tooth-shaped plasmonic waveguide filters with nanometeric sizes," Opt. Lett. **33**(23), 2874–2876 (2008).
16. J. Tao, X. G. Huang, X. Lin, Q. Zhang, and X. Jin, "A narrow-band subwavelength plasmonic waveguide filter with asymmetrical multiple-teeth-shaped structure," Opt. Express **17**(16), 13989–13994 (2009).
17. S. S. Xiao, L. Liu, and M. Qiu, "Resonator channel drop filters in a plasmon-polaritons metal," Opt. Express **14**(7), 2932–2937 (2006).

#129713 - $15.00 USD Received 8 Jun 2010; revised 17 Jul 2010; accepted 26 Jul 2010; published 5 Aug 2010

(C) 2010 OSA

18. A. Hosseini, and Y. Massoud, "Nanoscale surface Plasmon based resonator using rectangular geometry," Appl. Phys. Lett. **90**(18), 181102 (2007).
19. T. B. Wang, X. W. Wen, C. P. Yin, and H. Z. Wang, "The transmission characteristics of surface plasmon polaritons in ring resonator," Opt. Express **17**(26), 24096–24101 (2009).
20. A. Noual, A. Akjouj, Y. Pennec, J. Gillet, and B. Djafari-Rouhani, "Modeling of two-dimensional nanoscale Y-bent plasmonic waveguides with cavities for demultiplexing of the telecommunication wavelengths," N. J. Phys. **11**(10), 103020 (2009).
21. A. Taflove, and S. C. Hagness, "Computational Electrodynamics: The Finite-Difference Time-Domain Method," 2nd ed. 2000 (Artech House, Boston).
22. Z. H. Han, E. Forsberg, and S. He, "Surface plasmon Bragg gratings formed in metal-insulator-metal waveguides," IEEE Photon. Technol. Lett. **19**(2), 91–93 (2007).
23. S. L. Qiu, and Y. P. Li, "Q-factor instability and its explanation in the staircased FDTD simulation of high-Q circular cavity," J. Opt. Soc. Am. B **26**(9), 1664–1674 (2009).
24. I. Chremmos, "Magnetic field integral equation analysis of interaction between a surface plasmon polariton and a circular dielectric cavity embedded in the metal," J. Opt. Soc. Am. A **26**(12), 2623–2633 (2009).
25. Q. Li, T. Wang, Y. K. Su, M. Yan, and M. Qiu, "Coupled mode theory analysis of mode-splitting in coupled cavity system," Opt. Express **18**(8), 8367–8382 (2010).
26. Z. J. Zhong, Y. Xu, S. Lan, Q. F. Dai, and L. J. Wu, "Sharp and asymmetric transmission response in metal-dielectric-metal plasmonic waveguides containing Kerr nonlinear media," Opt. Express **18**(1), 79–86 (2010).

1. Introduction

Surface plasmon polaritons (SPPs) are waves trapped on the surfaces of metals owing to the interaction between the free electrons in metal and electromagnetic field in dielectric, and attenuating exponentially in the direction perpendicular to the interface [1,2]. SPPs have the most promising applications in the highly integrated optical circuits and devices due to their overcoming of diffraction limit and light manipulation on subwavelength scales [1, 3]. Recently, the devices based on SPPs, such as the all-optical switching [4–6], Mach-Zehnder interferometers [7], splitters [8], modulators [9], mirrors [10], sensors [11], and Bragg reflectors [12,13] are simulated numerically and demonstrated experimentally. Bragg reflectors are fabricated by alternatively stacking two kinds of dielectrics in metal-insulator-metal (MIM) or insulator-metal-insulator (IMI) plasmonic waveguides [12], and can realize the filtering functions. The IMI waveguide gives rise to less loss for the longer propagation distance, but fails to confine a light into subwavelength scale and, thus, is not suitable for high optical integration [14]. The MIM waveguide has a strong confinement of light and acceptable propagation length for SPPs [12].

Quite recently, some simple plasmonic waveguide filters have been proposed, such as tooth-shaped plasmonic waveguide filters [15,16], channel drop filters with disk resonators [17], rectangular geometry resonators [2, 18], and ring resonators [17, 19]. They overcome the complexity of fabrication of Bragg reflectors and decrease the prorogation length for SPPs. There exist two types of plasmonic filters in MIM waveguides, i.e., band-pass and band-stop filters. The band-stop filter prohibits light with certain frequency from propagating through the waveguide structures [15, 18]. The band-pass filter, which permits transmitting some frequency of light, is also very important in nanoscale optical devices [16, 19]. Some devices such as SPP reflectors need broad bandgaps [13]. In many cases such as wavelength division multiplexing (WDM) systems, however, narrow bandwidths are desired [16, 20].

In this paper, we propose a novel and simple plasmonic narrow-bandpass filter based on the MIM waveguide with a nanodisk resonator (i.e., disk-shaped naocavity). We focus on the tunable filtering characteristics of this filter structure. The wavelength-shift properties of resonant modes in the nanocavity calculated by the resonant theory of disk-shaped naocavity are validated by finite-difference time-domain (FDTD) method [21]. Another result obtained by FDTD simulations demonstrates that the bandwidths of resonance spectra can be manipulated by the coupling distance between the nanocavity and waveguides, which is analyzed exactly by temporal coupled mode theory.

#129713 - $15.00 USD Received 8 Jun 2010; revised 17 Jul 2010; accepted 26 Jul 2010; published 5 Aug 2010
(C) 2010 OSA

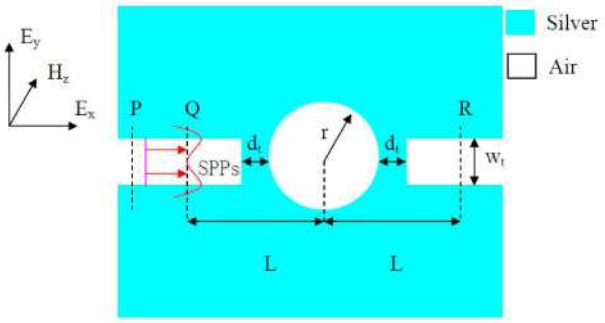

Fig. 1. Schematic diagram of the proposed plasmonic filter. r: radius of nanodisk resonator (disk-shaped nanocavity), w_t: metal slit width, d_t: coupling distance between the cavity and waveguides.

2. Structure and theories

Figure 1 shows the plasmonic filter structure which is composed of two slits, two semi-infinite metallic claddings, and a nanodisk resonator in the middle of the MIM structure. The insulators in the slit and cavity are set as air (n_d = 1). The metal is assumed as silver, whose complex relative permittivity can be characterized by the well-known Drude model [15]

$$\varepsilon_m(\omega)=\varepsilon_\infty-\frac{\omega_p^2}{\omega(\omega+i\gamma)}, \tag{1}$$

where ε_∞ is the dielectric constant at the infinite frequency, γ and ω_p are the electron collision frequency and bulk plasma frequency, respectively. ω is the angular frequency of incident light. The parameters for silver can be set as ε_∞ = 3.7, ω_p = 9.1 eV, and γ = 0.018 eV [22]. TM-polarized plane wave is emitted between the detective plane P and Q and propagates to R. The distance between P and Q is 10 nm. The distance between Q and R is 800 nm, i.e., L = 400 nm. The planes P, Q, and R detect the powers of internal field (i.e., P_P, P_Q, and P_R) respectively. $P_{in} = P_Q$-P_p presents the incident power, and $P_{out} = P_R$ denotes the transmission power. The transmission is defined as $T = P_{out}/P_{in}$ [15]. The exciting stable standing wave in the disk-shaped nanocavity forms the resonant condition [23,24] which can be given by

$$k_d\frac{H_n^{(1)'}(k_m r)}{H_n^{(1)}(k_m r)}=k_m\frac{J_n'(k_d r)}{J_n(k_d r)}, \tag{2}$$

where $k_{d,m} = k(\varepsilon_{d,m})^{1/2}$ are the wave vectors in the dielectric disk/metal, and r is the radius of the nanocavity. ε_d is the relative permittivity of the dielectric. ε_m stands for the relative permittivity of the metal, which is obtained from Eq. (1). k is the wave number and contains a relatively small negative imaginary part for a given n, where the negative imaginary part presents the loss [23]. J_n and J'_n are the first kind Bessel function with the order n and its derivation, $H_n^{(1)}$ and $H_n^{(1)'}$ are the first kind Hankel function with the order n and its derivation, respectively. The first and second-order modes are considered in the present paper, which correspond to the first and second order of Bessel and Hankel functions. From Eq. (2) we can see that the resonance wavelength λ_0 is dominated by r and the refractive index n_t (i.e., $(\varepsilon_d)^{1/2}$). The transmission spectra near the resonant modes in our system can be described by the temporal coupled mode theory, and the transmission T can be derived form Ref [25]. and described as

$$T(w)=\frac{(1/\tau_w)^2}{(w-w_0)^2+(1/\tau_i+1/\tau_w)^2}, \tag{3}$$

#129713 - $15.00 USD Received 8 Jun 2010; revised 17 Jul 2010; accepted 26 Jul 2010; published 5 Aug 2010
(C) 2010 OSA

where w is the frequency of incident light, and w_0 presents the resonance frequency. $1/\tau_i$ and $1/\tau_w$ stand for the decay rate of the field induced by the internal loss in the nanocavity and the power escape through the waveguides, respectively. At the resonance frequency w_0, the cavity mode is excited and the incident light is transmitted. Far from the resonance frequency, the incident mode is completely reflected. When $1/\tau_i$ is far less than $1/\tau_w$, the on-resonance transmission (i.e., transmission peak) $T_{max} = (1/\tau_w)^2/(1/\tau_w + 1/\tau_i)^2$ is close to unity. From Eq. (3), we can find that the transmission spectra around the resonant modes exhibit Lorentzian profiles.

3. Simulation results and analysis

The parameters of the filter structure are set as r = 200 nm, w_t = 50 nm, d_t = 20 nm, and L = 400 nm. Firstly, we utilize the FDTD method to simulate the transmission characteristics. Figure 2(a) shows the transmission spectrum including the two low-order modes (Mode 1 and 2) observed in the visible and near-infrared spectral range. The transmission exhibits evident filtering property at the two modes. The transmission peaks do not reach unity due to the internal loss in the nanocavity as well as waveguide loss in the metal slits. The transmission response exhibits Lorentzian shape, which is in accordance with above theoretic analysis. Field distributions of $|H_z|$ at the incident wavelength of 520 nm (i.e., Mode 1), the wavelength of 700 nm, and the wavelength of 816 nm (i.e., Mode 2) are depicted in Figs. 2(b)-(d), respectively. It is found that the excitations of resonant modes emerge in the nanocavity at the wavelengths of 520 nm and 816 nm, where the incident light can pass through the MIM plasmonic structure. In addition, there exists no excitation of resonant mode when the wavelength is 700 nm, where the propagation of the incident light is stopped. As shown in Fig. 2(a), the transmission at resonant mode 2 has higher coefficient than that of mode 1. This may be due to that resonant mode 2 has larger $1/\tau_w$ than mode 1.

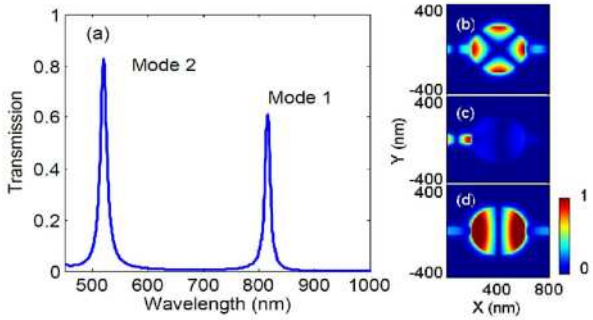

Fig. 2. (a) Transmission spectrum with the original parameters of configuration. The corresponding normalized field distributions of $|H_z|$ with wavelengths of (b) 520 nm (Media 1), (c) 700 nm (Media 2), and (d) 816 nm (Media 3) exhibit respective transmission characteristics.

Successively, we investigate the influence of the radius of the nanocavity on the resonance wavelengths first by the FDTD method and then by the resonant mode theory. The radius is set as variable while the other parameters are fixed as above. Figure 3(a) shows the transmission response of SPPs corresponding to different radius. The resonance wavelengths have a red-shift with increasing of the radius. Figure 3(b) reveals that the wavelength-shifts of the resonant modes 1 and 2 almost have approximately linear relations with the radius of nanocavity. This result is in accordance with the solution of Eq. (2). According to the simulations and analysis above, it is seen that the band-pass filter can be easily tuned by changing the radius of nanocavity. We have known that the resonant modes are influenced by the refractive index of the material filling the nanocavity. Thus, we can manipulate the wavelengths of resonant modes by changing the value of refractive index (n_t) in the nanocavity. The other parameters are set as above. Figure 4(a) shows the transmission spectra with different refractive index of the nanocavity. From Fig. 4(b) we find that the red-shifts of

#129713 - $15.00 USD Received 8 Jun 2010; revised 17 Jul 2010; accepted 26 Jul 2010; published 5 Aug 2010
(C) 2010 OSA

resonance wavelengths have nearly linear relations with n_t. The results from the resonant theory of disk-shaped nanocavity are consistent with those obtained by FDTD simulations. Therefore, one can fill some dielectric material into the nanocavity to design the band-pass plasmonic filter with demanded channel.

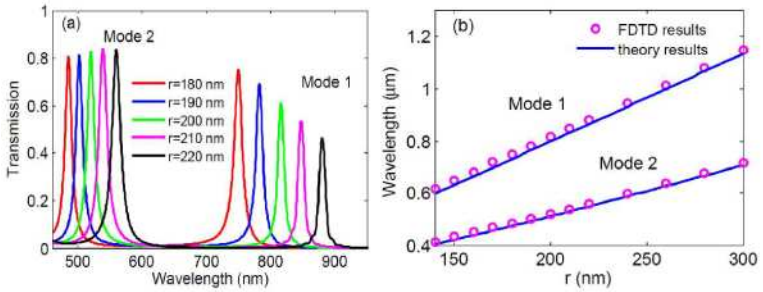

Fig. 3. (a) Transmission spectra with different radii of the nanocavity. (b) Relationship between resonance wavelengths and the radius of the cavity.

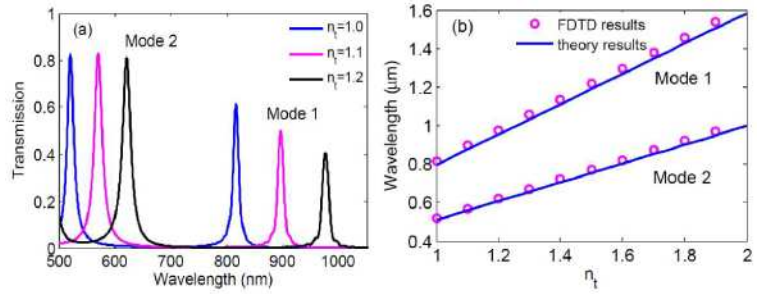

Fig. 4. (a) Transmission spectra with different refractive index. (b) Relationship between resonance wavelengths and the refractive index.

Another structure parameter d_t, which stands for the coupling distance between the nanodisk resonator and the waveguides, is an important factor influencing the intensities of transmission spectra near the resonant modes. The decay rate $1/\tau_i$ keeps approximately unchanging when only d_t is changed. Meanwhile, the decay rate $1/\tau_w$ will intensively decrease when d_t is increased from zero to tens of nanometers. The on-resonance transmission $T_{max} = (1/\tau_w)^2/(1/\tau_w + 1/\tau_i)^2$ will accordingly decrease. The results are verified by FDTD simulations, as shown in Figs. 5(a) and (b). The resonance wavelengths exhibit slight blue-shift for larger coupling distances, which is consistent with the results in Ref [19]. According to Eq. (3), full width at half maximum of the resonance spectrum $\Delta_{FWHM} \approx 4\pi c(1/\tau_w + 1/\tau_i)/w_0^2$ will intensively decrease along with $1/\tau_w$, as shown in Fig. 5(a). Therefore, the bandwidths of the resonance spectra can be tuned by controlling the coupling distance.

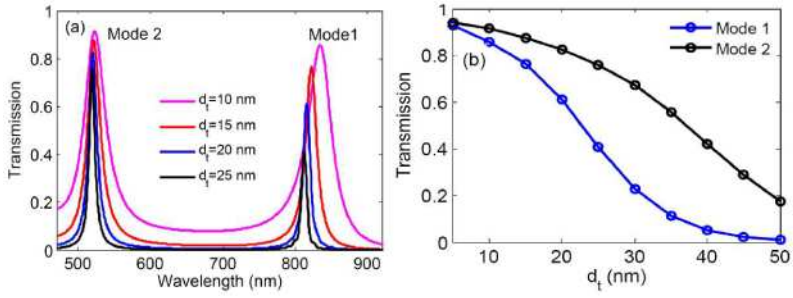

Fig. 5. (a) Transmission spectra with different d_t. (b) Relationship between the on-resonance transmissions and d_t. The other parameters are set as original values.

#129713 - $15.00 USD Received 8 Jun 2010; revised 17 Jul 2010; accepted 26 Jul 2010; published 5 Aug 2010
(C) 2010 OSA

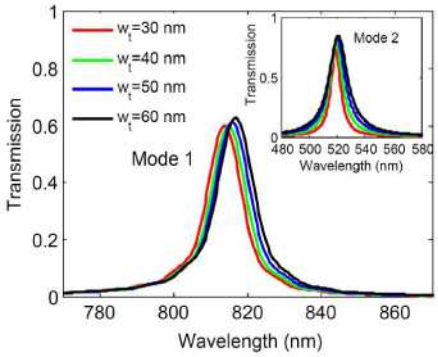

Fig. 6. Transmission spectra with different metal slit widths in the MIM waveguides.

Finally, we study the influence of the metal slit width w_t on the transmission characteristics of SPPs. Since w_t is usually set as tens of nanometers [19, 26], here the situations of w_t = 30, 40, 50, and 60 nm are considered for simulation. Figure 6 shows the transmission spectra with different slit widths. It is found that the transmission spectrum fluctuates quite slightly, while shows a little red-shift and height-rise which can be attributed to the waveguide loss [26].

4. Conclusion

In this paper, a simple and ease of fabrication plasmonic filter based on MIM waveguides with a nanodisk resonator is proposed. The resonant modes are calculated by the resonant theory of disk-shaped nanocavity, and we find that the central wavelengths of the resonance transmission can be easily controlled by modulating the radius and refractive index of the nanocavity. The results are in good agreement with that obtained by the FDTD method. Furthermore, it is shown that the bandwidths of resonance spectra can be tuned by adjusting the coupling distance between the nanocavity and waveguides. This result achieved by FDTD simulations can be accurately analyzed by temporal coupled mode theory. This ultra-compact structure has extensive potential in nanoscale integrated optical circuits due to its simplicity for design of tunable narrow band-pass filters.

Acknowledgments

This work was supported by the National Natural Science Foundation of China under Grant 10874239 and 10604066. The authors would especially like to thank Mr. Miao Feng for help with the FDTD method.

Corresponding author (X. Liu). Tel.: + 862988881560; fax: + 862988887603; electronic mail: liuxueming72@yahoo.com and liuxm@opt.ac.cn.

#129713 - $15.00 USD Received 8 Jun 2010; revised 17 Jul 2010; accepted 26 Jul 2010; published 5 Aug 2010
(C) 2010 OSA